



Functional Evaluation of Retinal Pigment Epithelium and Outer Retinal Atrophy by High-Density Targeted Microperimetry Testing

Zhichao Wu, BAppSc(Optom), PhD,^{1,2} Emily K. Glover, OD,¹ Erin E. Gee, BAppSc(MedRad),¹ Lauren A.B. Hodgson, MPH,¹ Robyn H. Guymer, MBBS, PhD^{1,2}

Purpose: Complete retinal pigment epithelium (RPE) and outer retinal atrophy (cRORA) on OCT imaging has recently been proposed to describe end-stage atrophy in age-related macular degeneration (AMD) by international consensus and expected to be associated with a *dense scotoma*, but such functional evidence is lacking. This study sought to examine the visual sensitivity defects associated with cRORA and to determine OCT features associated with deep defects.

Design: Observational study.

Participants: Sixty eyes from 53 participants, including 342 microperimetry tests over 171 study visits.

Methods: Participants underwent targeted high-density threshold-based microperimetry testing of atrophic lesions (with at least incomplete RPE and outer retinal atrophy [iRORA]) with a 3.5° diameter grid. The maximum extent of signs of atrophy for all lesions was graded on OCT imaging.

Main Outcome Measures: Number of deep visual sensitivity defects (threshold ≤ 10 decibels [dB]).

Results: Presence of choroidal signal hypertransmission $\geq 500 \mu\text{m}$, complete RPE loss $\geq 250 \mu\text{m}$, and inner nuclear layer and outer plexiform layer subsidence, and hyporeflective wedge-shaped band (defined as nascent geographic atrophy [nGA]) $\geq 500 \mu\text{m}$ ($P \leq 0.020$), but not RPE attenuation or disruption ($P \geq 0.192$), were all independently associated with a significant increase in the number of deep visual sensitivity defects ≤ 10 dB. Only cRORA lesions with hypertransmission $\geq 500 \mu\text{m}$ or complete RPE loss $\geq 250 \mu\text{m}$, or with both of these features ($P < 0.001$), but not lesions with only hypertransmission 250–499 μm ($P = 0.303$), had significantly more deep visual sensitivity defects ≤ 10 dB compared with iRORA lesions. Lesions with nGA $\geq 500 \mu\text{m}$, irrespective of the presence of hypertransmission $\geq 500 \mu\text{m}$ and/or complete RPE loss $\geq 250 \mu\text{m}$, also showed a higher number of deep visual sensitivity defects ≤ 10 dB compared with lesions without nGA $\geq 500 \mu\text{m}$ ($P \leq 0.011$).

Conclusions: Not all cRORA lesions show a difference in the number of deep visual sensitivity defects compared with iRORA. Instead, hypertransmission $\geq 500 \mu\text{m}$, complete RPE loss $\geq 250 \mu\text{m}$, and nGA $\geq 500 \mu\text{m}$ are all OCT features independently associated with deep visual sensitivity defects that could help inform the definition of end-stage atrophy on OCT imaging.

Financial Disclosure(s): Proprietary or commercial disclosure may be found in the Footnotes and Disclosures at the end of this article. *Ophthalmology Science* 2024;4:100425 © 2023 by the American Academy of Ophthalmology. This is an open access article under the CC BY-NC-ND license (<http://creativecommons.org/licenses/by-nc-nd/4.0/>).



Supplemental material available at www.opthalmologyscience.org.

OCT is a technique that enables depth-resolved imaging of the retina at near-cellular resolution, allowing the characteristic features of retinal pigment epithelium (RPE) loss and overlying photoreceptor degeneration associated with geographic atrophy (GA)^{1–5} in age-related macular degeneration (AMD) to be visualized.^{6–9} In recent years, an international group of AMD and retinal imaging experts, called the Classification of Atrophy Meetings group, was formed and sought to provide a lexicon to describe OCT-defined features of atrophy through international

consensus.^{10,11} This OCT-based classification was intended to unite the field moving forward by providing common nomenclature and to provide a more granular classification system by describing both end-stage atrophy and its precursors.

The Classification of Atrophy Meetings group proposed an OCT classification system wherein end-stage atrophy was defined as *complete RPE and outer retinal atrophy* (cRORA), based on the presence of choroidal signal hypertransmission $\geq 250 \mu\text{m}$, associated with RPE

attenuation or disruption $\geq 250 \mu\text{m}$ and evidence of overlying photoreceptor degeneration.¹⁰ The OCT changes presumed to portend the development of cRORA were defined as incomplete RPE and outer retinal atrophy (iRORA), which were defined as regions with the same features that defined cRORA but where the choroidal signal hypertransmission and/or the RPE attenuation or disruption were $< 250 \mu\text{m}$.¹¹ The Classification of Atrophy Meetings group suggested that “one might expect to have a dense scotoma if it were possible to test only the area of cRORA, [and] that one might expect that areas of iRORA would retain some degree of retinal sensitivity (relative scotoma).”¹⁰

Fundus-tracked perimetry (or microperimetry) is a technique that enables measurements of visual sensitivity at specific retinal locations,^{12,13} and previous studies in eyes with GA have reported that visual sensitivity loss at specific locations sampled on microperimetry was associated with changes in the RPE and/or photoreceptors seen on OCT imaging.^{14–18} However, no studies to date have specifically examined whether regions with cRORA are characterized by the presence of dense scotoma(s) or deep visual sensitivity defect(s) or determined the association between the presence and extent of OCT signs of atrophy with such deep visual sensitivity defects.

This study thus sought to comprehensively evaluate regions with at least iRORA using a high-density, targeted microperimetry testing approach to understand the association between the presence and extent of OCT signs of atrophy with deep visual sensitivity defects. This evaluation will provide evidence for whether regions with cRORA are characterized by having deep visual sensitivity defect(s)¹⁰ and also determine what OCT-defined changes are present when such deep visual sensitivity defect(s) are observed. One such OCT-defined change of interest is *nascent geographic atrophy* (nGA),^{19–21} specific features of photoreceptor degeneration associated with a high risk of progression to end-stage GA,^{22–24} which was also examined for its association with deep visual sensitivity defects in this study.

Methods

This study included individuals who were enrolled in a prospective observational study of early OCT atrophic changes undertaken at the Centre for Eye Research Australia. This study was conducted in accordance with the tenets of the Declaration of Helsinki and the International Conference on Harmonization Guidelines for Good Clinical Practice. Institutional review board approval was obtained for this study, and all the enrolled participants provided informed consent.

Participants

This study included individuals who were aged ≥ 50 years who had at least iRORA secondary to AMD and a best-corrected visual acuity of 20/100 or better, without evidence of neovascular AMD or having undergone treatments previously, in ≥ 1 eye. Additionally, individuals with any ocular, systemic, or neurologic condition(s) that may prohibit a reliable assessment of the retina and/or visual function (such as significant media opacities or

glaucoma) were excluded from this study. As per previous reports,^{11,24} iRORA was defined by the presence of choroidal signal hypertransmission associated with RPE attenuation or disruption, either of which is $< 250 \mu\text{m}$, and with evidence of overlying photoreceptor degeneration. The evidence of photoreceptor degeneration included the presence of ellipsoid zone (EZ) or external limiting membrane (ELM) disruption, outer nuclear layer (ONL) thinning, subsidence of the inner nuclear layer (INL) and outer plexiform layer (OPL), or presence of a hyporeflexive wedge-shaped band within Henle’s fiber layer.^{11,24} Participants with iRORA were included in this study to serve as a reference group when evaluating the associations with deep visual sensitivity defects in regions with more progressed atrophic changes.

Participants in the prospective observational study were first seen at 1 visit to perform microperimetry testing of 1 eligible study eye, and those deemed to also have nGA^{19–21,25} or more progressed atrophic changes in the eligible eye(s) at baseline were also offered an opportunity to undergo longitudinal follow-up testing at 3-monthly intervals for up to 12 months, due to our interest in further understanding progressive visual function loss in regions with nGA. As described in previous studies,^{19–21,23} nGA is defined by the presence of subsidence of the INL and OPL, and/or presence of a hyporeflexive wedge-shaped band within Henle’s fiber layer. Note that these features that define nGA represent only a subset of all the possible features that could be used to define the presence of photoreceptor degeneration required in the criteria for iRORA, as defined here. This means that it is not mandatory for features of nGA to be present when defining the presence of iRORA, and vice versa, although a lesion could meet the definition of having both iRORA and nGA. Note, however, that there were no cases in this study with nGA without iRORA, as all eyes were required to have iRORA in this study. All participants were offered an opportunity to undergo microperimetry testing of both eyes during different study visits if both eyes met the eligibility criteria of this study.

Retinal Imaging

Macular-centered OCT volume scans sampling a $20^\circ \times 20^\circ$ region were acquired on the Spectralis HRA+OCT device (Heidelberg Engineering GmbH) and consisted of 97 B-scans (1024 A-scans each, with an automatic real-time averaging of 16 frames). Macular-centered color fundus photographs were also acquired using the Canon CR6-45NM device (Canon), covering a 45° diameter region.

Microperimetry Testing

Microperimetry testing was performed using the Macular Integrity Assessment (MAIA) device (CenterVue) before any assessments that could bleach the retina or affect the ocular surface and after pupillary dilation. The MAIA device captures $36.5^\circ \times 36.5^\circ$ fundus images at 25 frames per second using a line-scanning laser ophthalmoscope (central wavelength = 850 nm) to perform fundus-tracking during testing. Visual sensitivities were measured using Goldman Size III stimuli (0.43° diameter; luminance range = $1.35\text{--}318 \text{ cd/m}^2$) against an achromatic background (luminance = 1.27 cd/m^2 ; dynamic range = 36 decibels [dB] of differential contrast), using a 4-2 staircase threshold strategy and with a 1° diameter red central fixation target.

Testing was performed using an isotropic stimulus pattern consisting of 37 points that sampled a 3.5° diameter region ($1000 \mu\text{m}$ approximately; interstimulus spacing = 0.5°), manually repositioned and centered on an atrophic lesion of interest. Only lesions that were smaller than the stimulus pattern (approximately ≤ 750

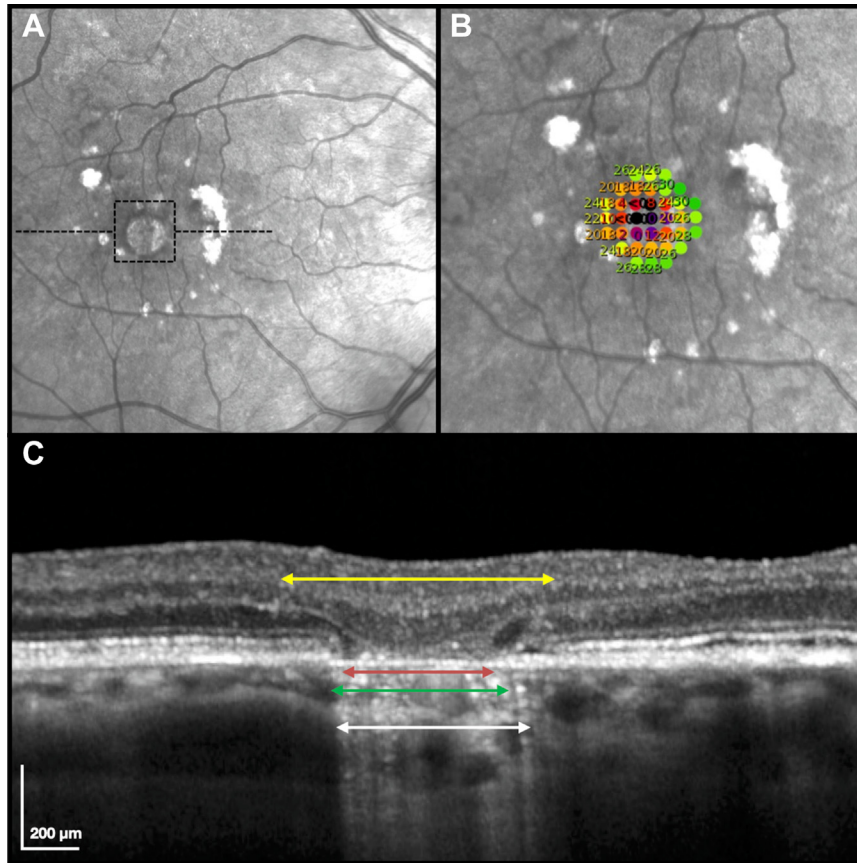


Figure 1. Example of an eye with complete retinal pigment epithelium (RPE) and outer retinal atrophy that underwent high-density targeted microperimetry testing in this study, with the region tested outlined by a dashed box (A) and shown with a magnified view with the stimulus pattern overlaid on the near-infrared reflectance image (B); numbers shown represent visual sensitivity in decibels). An OCT B-scan taken through this atrophic lesion (location as outlined by the black dashed horizontal lines on the (A) is also shown (C). The extent of atrophic changes that were measured in this study are shown on this B-scan, including the choroidal signal hypertransmission (white double arrows), RPE attenuation or disruption (green double arrows), complete RPE loss (red double arrows), and subsidence of the inner nuclear layer and outer plexiform layer and/or hyporeflective wedge-shaped band within Henle's fiber layer (yellow double arrows; i.e., the extent of this feature was defined by the limits of either of these features).

μm in diameter, so that the stimulus pattern also sampled non-atrophic regions) were included in this study. When multiple atrophic lesions were present in an eye, only the lesion(s) that were isolated from other lesions were considered eligible (so that the stimulus pattern only sampled 1 atrophic lesion), and the lesion with the most definite features of nGA was chosen for testing. An example of the stimulus pattern used in this study is shown in Figure 1. All tests were manually reviewed after the completion of the first microperimetry test to ensure that the atrophic lesion was sampled entirely by the stimulus grid.

Testing with this high-density targeted microperimetry approach was performed ≥ 3 times at the first visit, with each subsequent test from the first test performed using the “follow-up” function at the same visit. This was performed to minimize potential learning effects²⁵ and/or the systematic underestimation of visual sensitivity losses on the first test,²⁶ which was excluded from the analyses in this study. For participants who were seen at subsequent visit(s), the “follow-up” function was also used so that testing was performed at the same retinal location at baseline, and ≥ 2 tests were performed at these subsequent visits. Participants were always offered a few minutes of rest between each microperimetry test to minimize the potential effect

of fatigue. The reliability of each test at all visits was assessed by false-positive catch trials through presenting suprathreshold stimuli at the optic nerve head, and tests with $> 25\%$ false-positive errors were considered unreliable and repeated where possible.

The primary aim of this study was to understand if regions of cRORA are characterized by the presence of dense scotoma(s), and also determine the OCT imaging features associated with the presence of such dense scotoma(s). However, dense scotomas, or *absolute* scotomas, are typically defined as locations of non-response to the brightest presentable stimuli (or 0 dB),²⁷ and the luminance of this brightest stimuli depends on the physical dynamic range of the device used.^{28,29} However, this physical dynamic range does not always correspond to the limits of human perception or the effective dynamic range.³⁰ A previous study has shown that the floor of the effective dynamic range of the MAIA device used in this study, defined as locations where 5% of the retest values include 0 dB (i.e., deemed to be indistinguishable from the floor of the physical dynamic range statistically), was 10 dB.³¹ We thus sought to evaluate the number of test locations with a visual sensitivity threshold of ≤ 10 dB and ≤ 0 dB, and termed locations with such values as having “deep visual sensitivity defects.” They represent locations

that fall well outside the range of normal visual sensitivities³¹ and correspond to values at the floor of the effective and physical dynamic range, respectively.

Image Grading

The atrophic lesions that underwent high-density targeted microperimetry testing were graded on the OCT B-scans by 2 senior graders together (R.H.G. and Z.W., who resolved any disagreements immediately through open adjudication) while masked to the microperimetry testing results. Each lesion was first independently assessed to confirm the presence of at least iRORA.^{11,24} The maximum width, along any of the horizontal OCT B-scans that sampled the atrophic lesion that underwent microperimetry testing, of the following features used to define RPE and outer retinal atrophy were then measured: (1) choroidal signal hypertransmission (based on its full extent that was attributable to a single lesion, irrespective of the degree of interruption[s] in its continuity), (2) RPE attenuation or disruption, (3) complete RPE loss (defined when there was a bare Bruch's membrane, without overlying debris or dysmorphic RPE), and (4) subsidence of the INL and OPL, and/or hyporeflective wedge-shaped band (meeting the definition of having nGA). Note that measurements of the extent of RPE attenuation or disruption included regions with complete RPE loss. An example of the extent of these 4 features measured along an OCT B-scan is also shown in Figure 1.

Statistical Analyses

The association between the number of test locations (from the 37 locations tested) with a deep visual sensitivity defect (i.e., locations with a sensitivity of ≤ 10 dB or ≤ 0 dB) and the extent of the OCT features of atrophy were measured using multivariable linear mixed models to account for the correlations between 2 tests that were performed at a visit, multiple testing visits for an eye, and 2 eyes within each participant. The extent of the abovementioned 4 OCT features of atrophy was grouped into approximately 250- μ m bins (1–249 μ m, 250–499 μ m, etc.) for the analyses, and any categories with few observations ($n \leq 5$) were collapsed with an adjacent category. These multivariable models were adjusted for the confounder of participant age.

The OCT features identified as being associated with deep visual sensitivity defects were then used in different combinations that produced different categories of atrophic lesions, as described in the Results section. The differences in the number of deep visual sensitivity defects across these categories within each combination were also compared using similar linear mixed models, also adjusting for the age of the participants. These analyses were all conducted using Stata/IC (software version 16; StataCorp).

Results

A total of 60 eyes from 53 participants were included in this study, and these participants were on average 75 ± 8 years old (range, 53–86 years), and 39 (74%) participants were female. These eyes underwent testing over a median of 2 visits (interquartile range = 1–5 visits). As such, a total of 171 study visits were included in this study from all participants, consisting of 342 high-density targeted microperimetry tests (as 2 tests from each visit were included). At the first visit of each eye, 15 (25%) and 45 (75%) lesions tested had iRORA and cRORA, respectively. There were

also a total of 47 (78%) lesions tested with nGA, which were present in 12 (80%) and 35 (78%) of the eyes with iRORA and cRORA, respectively.

Association between OCT Signs of Atrophy with Deep Visual Sensitivity Defects

The associations between the number of deep visual sensitivity defects ≤ 10 dB and ≤ 0 dB separately with each individual OCT feature of atrophic AMD, evaluated in 250- μ m bins, are presented in Table 1. It showed that the presence of hypertransmission 500–1000 μ m ($P \leq 0.033$), but not 250–499 μ m ($P \geq 0.584$), was associated with a significantly larger number of locations with deep visual sensitivity defects that were ≤ 10 dB and ≤ 0 dB when compared with the presence of hypertransmission 1–249 μ m. Neither the presence of RPE attenuation or disruption 500–750 μ m or 750–1000 μ m was associated with a significantly larger number of locations with deep visual sensitivity defects ≤ 10 dB or ≤ 0 dB compared with the presence of RPE attenuation or disruption 1–499 μ m ($P \geq 0.192$). However, the presence of complete RPE loss 250–750 μ m ($P < 0.001$), but not 1–249 μ m ($P \geq 0.239$), was associated with a significantly larger number of locations with deep visual sensitivity defects that were ≤ 10 dB and ≤ 0 dB when compared with the absence of complete RPE loss. Finally, it showed that the presence of subsidence of the INL and OPL, or hyporeflective wedge-shaped band(s) within HFL (2 features that define nGA), with an extent of 500–749 μ m and 750–1000 μ m ($P \leq 0.020$), but not 1–249 μ m and 250–499 μ m ($P \geq 0.635$) was significantly associated with a larger number of test locations ≤ 10 dB compared with their absence. In addition, the presence of INL and OPL subsidence, or hyporeflective wedge-shaped band(s), with an extent of 750–1000 μ m was significantly associated with a larger number of deep visual sensitivity defects that were ≤ 0 dB compared with when they were absent ($P = 0.002$) but not when their extents were 1–249 μ m, 250–499 μ m, and 500–749 μ m ($P \geq 0.501$).

These findings suggest that the presence of hypertransmission ≥ 500 μ m, complete RPE loss ≥ 250 μ m, and nGA (subsidence of the INL and OPL, or hyporeflective wedge-shaped band) ≥ 750 μ m are all OCT features that were independently associated with deep visual sensitivity defects ≤ 10 dB and ≤ 0 dB, and nGA ≥ 500 μ m was also significantly associated with deep visual sensitivity defects ≤ 10 dB. Differences in the extent of deep visual sensitivity defects present, based on combinations of these 3 features were thus explored. The first set of combinations explored, involved 4 categories using features that relate to the definition of RPE and outer retinal atrophy (noting that the lesions were always assigned the highest category that it met the criteria for):

1. Category 1: any hypertransmission associated with any RPE attenuation or disruption and evidence of overlying photoreceptor degeneration (meeting the definition of iRORA)

Table 1. Association between the Extent of Individual OCT Signs of Atrophy and the Number of Test Locations on Microperimetry with Deep Visual Sensitivity Defects (Examined Separately for Sensitivity of ≤ 10 dB or ≤ 0 dB)

Parameter	n	No. Locations ≤ 10 dB		No. Locations ≤ 0 dB	
		Coefficient (95% CI)	P Value	Coefficient (95% CI)	P Value
Choroidal signal hypertransmission					
1–249 μm	28	Reference	–	Reference	–
250–499 μm	107	0.1 (–0.7 to 0.8)	0.827	–0.1 (–0.5 to 0.3)	0.584
500–750 μm	32	2.3 (1.2 to 3.4)	< 0.001	0.6 (0.0 to 1.1)	0.033
750–1000 μm	4*				
RPE attenuation or disruption					
1–249 μm	2*	Reference	–	Reference	–
250–499 μm	26				
500–750 μm	43	–0.1 (–0.9 to 0.7)	0.749	0.0 (–0.4 to 0.4)	0.904
750–1000 μm	100	0.5 (–0.3 to 1.3)	0.192	0.1 (–0.3 to 0.5)	0.579
Complete RPE loss [†]					
None	88	Reference	–	Reference	–
1–249 μm	63	0.4 (–0.2 to 0.9)	0.239	0.1 (–0.2 to 0.4)	0.511
250–499 μm	16	3.9 (2.8 to 4.9)	< 0.001	1.4 (0.8 to 1.9)	< 0.001
500–750 μm	4*				
Subsidence of the INL and OPL, or hyporeflective wedge-shaped band					
None	22	Reference	–	Reference	–
1–249 μm	8	–0.1 (–1.5 to 1.3)	0.924	–0.2 (–0.9 to 0.5)	0.542
250–499 μm	58	0.3 (–0.8 to 1.3)	0.635	–0.2 (–0.6 to 0.3)	0.501
500–750 μm	57	1.3 (0.2 to 2.5)	0.020	0.2 (–0.3 to 0.7)	0.517
750–1000 μm	26	2.6 (1.2 to 4.0)	< 0.001	1.1 (0.4 to 1.7)	0.002

CI = confidence interval; dB = decibels; INL = inner nuclear layer; n = number of visits; No. = number; OPL = outer plexiform layer; RPE = retinal pigment epithelium.

*Collapsed with the adjacent category due to small number of visits with this feature present ($n \leq 5$).

[†]Resulting in the clear visibility of Bruch's membrane and without overlying dysmorphic RPE or debris present. Note that all analyses were adjusted for the age of the participant.

- Category 2: as per category 1, but with hypertransmission ≥ 250 μm associated with RPE attenuation or disruption ≥ 250 μm and evidence of overlying photoreceptor degeneration (meeting the definition of cRORA)
- Category 3: as per category 2, but with either hypertransmission ≥ 500 μm or complete RPE loss ≥ 250 μm
- Category 4: as per category 3, but with both hypertransmission ≥ 500 μm and complete RPE loss ≥ 250 μm

With this first set of combinations, the number of locations with deep visual sensitivity defects that were ≤ 10 dB or ≤ 0 dB was significantly higher for lesions in categories 3 and 4 ($P < 0.001$ for all), but not category 2 ($P \geq 0.303$), when compared with category 1. Lesions in categories 3 and 4 also had a significantly higher number of deep visual sensitivity defects ≤ 10 dB and ≤ 0 dB compared with lesions in categories 2 and 3, respectively (i.e., their lower neighboring category; $P < 0.001$ for all). These findings are all presented graphically in Figure 2A. Note that hypertransmission ≥ 500 μm was present more frequently than complete RPE loss ≥ 250 μm for lesions in category 3 (adjusted prevalence = 76% and 24%, respectively).

The second set of combinations explored also involved 4 categories, but instead corresponded to the number of the 3

features reported here associated with deep visual sensitivity defects that were ≤ 10 dB (i.e., hypertransmission ≥ 500 μm , complete RPE loss ≥ 250 μm , and nGA ≥ 500 μm). In other words, categories 1, 2, 3, and 4 correspond to requiring none, 1 of any, 2 of any, and all 3 of these features to be present, respectively. With this second set of combinations, the number of locations with deep visual sensitivity defects that were ≤ 10 dB or ≤ 0 dB also was significantly higher for lesions in categories 3 and 4 when compared with category 1 ($P < 0.001$ for all). Lesions in categories 3 and 4 also had a significantly higher number of deep visual sensitivity defects ≤ 10 dB and ≤ 0 dB compared with lesions in categories 2 and 3, respectively ($P < 0.001$ for all). For lesions in category 2, there was a significantly higher number of locations ≤ 10 dB ($P = 0.022$), but not ≤ 0 dB ($P = 0.204$), when compared with category 1. These findings are presented graphically in Figure 2B.

Note that with the aforementioned second set of combinations, nGA ≥ 500 μm was one of the 3 features most frequently present in category 2 lesions (adjusted prevalence = 92%), followed equally by hypertransmission ≥ 500 μm and complete RPE loss ≥ 250 μm (adjusted prevalence = 4% for both). For category 3 lesions, the 2 pairs of features most frequently present were nGA ≥ 500 μm and hypertransmission ≥ 500 μm (adjusted prevalence = 73%), followed by nGA ≥ 500 μm and complete RPE loss ≥ 250 μm (adjusted prevalence = 27%).

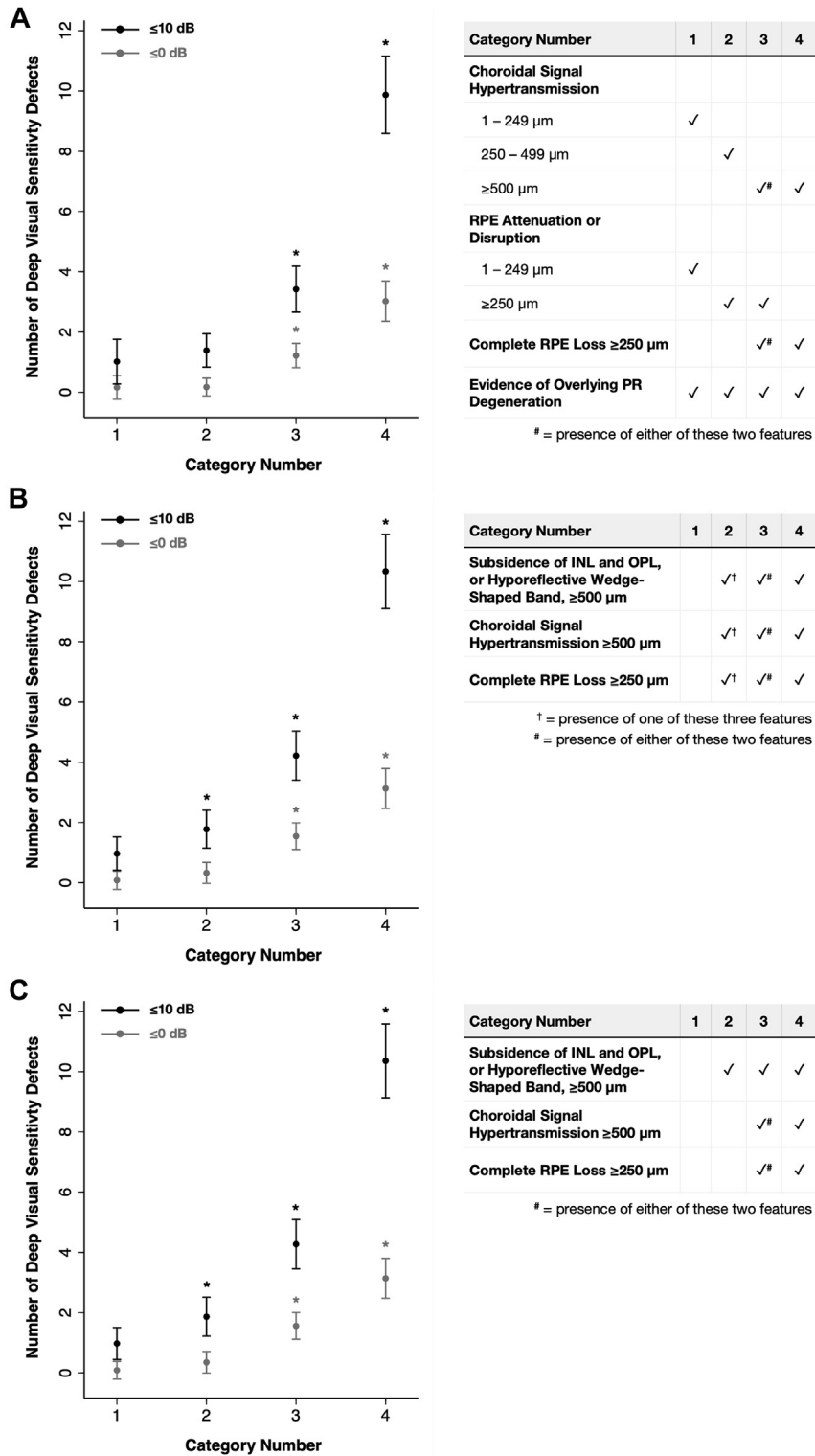


Figure 2. Differences in the mean number of microperimetry test locations (from 37 locations tested) with a deep visual sensitivity defect (based on being ≤ 10 decibels [dB] or ≤ 0 dB; black and gray markers, respectively), based on 3 different sets of combinations of OCT features (left). Each set of combinations (A, B, and C) involved 4 categories, and the criteria for meeting each category are indicated in their respective tables (right; “✓” = required feature); lesions were always assigned the highest category that it met the criteria for. * = statistically significant at $P < 0.05$ compared with category 1 or each category compared with their lower neighboring category (e.g., category 4 compared with category 3). INL = inner nuclear layer; OPL = outer plexiform layer; PR = photoreceptor; RPE = retinal pigment epithelium.

As such, this second set of combinations could be simplified into the following 4 categories based upon the much higher prevalence of nGA in the sample (with lesions always assigned the highest category that it met the criteria for):

1. Category 1: any lesion not meeting the criteria for the other categories
2. Category 2: presence of nGA $\geq 500 \mu\text{m}$
3. Category 3: as per category 2, but with either hypertransmission $\geq 500 \mu\text{m}$ or complete RPE loss $\geq 250 \mu\text{m}$
4. Category 4: as per category 3, but with both hypertransmission $\geq 500 \mu\text{m}$ and complete RPE loss $\geq 250 \mu\text{m}$

Findings for this third set of combinations were similar to those for the second set of combinations, where the number of locations with deep visual sensitivity defects that were ≤ 10 dB or ≤ 0 dB also was significantly higher for lesions in categories 3 and 4 when compared with category 1 ($P < 0.001$ for all). Similarly, lesions in categories 3 and 4 had a significantly higher number of deep visual sensitivity defects ≤ 10 dB and ≤ 0 dB compared with lesions in categories 2 and 3, respectively ($P < 0.001$ for all). However, lesions in category 2 also showed a significantly higher number of locations ≤ 10 dB ($P = 0.011$), but not ≤ 0 dB ($P = 0.168$), when compared with category 1. These findings are presented graphically in Figure 2C.

These aforementioned findings for the differences in the number of locations with deep visual sensitivity defects ≤ 10 and ≤ 0 dB based on the 3 different set of combinations of OCT features were also seen when evaluating the mean sensitivity (MS) of all the microperimetry test locations (Supplementary Materials, available at www.ophtalmology.org).

Examples of Study Findings

Six examples from this study of the high-density targeted microperimetry testing results of atrophic lesions that differed in their presence and extent of the OCT signs of atrophy are shown in Figure 3. The first example (Fig 3A) shows a lesion with iRORA, where deep visual sensitivity defects were absent, although some localized functional loss was present. The second example (Fig 3B) shows a lesion with cRORA without definite evidence of INL and OPL subsidence or a hyporeflective wedge-shaped band, where the choroidal signal hypertransmission was between 250–499 μm . Deep visual sensitivity defects ≤ 10 dB were also absent in association with this lesion, although local visual sensitivity losses were observed (2 locations ≤ 14 dB).

The third example (Fig 3C) shows a lesion with nGA, where the subsidence of the INL and OPL and/or hyporeflective wedge-shaped band, was between 500–749 μm , but this lesion did not have choroidal signal hypertransmission $\geq 250 \mu\text{m}$ (and would thus not have met the criteria for cRORA). There were 3 locations of deep visual sensitivity defects ≤ 10 dB associated with this lesion but no locations that were ≤ 0 dB. The fourth example (Fig 3D)

shows a lesion with cRORA, also satisfying the criteria for nGA, with both choroidal signal hypertransmission between 250–499 μm and subsidence of the INL and OPL, and/or hyporeflective wedge-shaped band that was between 500–749 μm . There were also 3 locations of deep visual sensitivity defects ≤ 10 dB but no locations that were ≤ 0 dB, associated with this lesion.

The fifth example (Fig 3E) shows a lesion with cRORA, also satisfying the criteria for nGA, that had a larger extent of choroidal signal hypertransmission between 500–749 μm , along with subsidence of the INL and OPL, and/or hyporeflective wedge-shaped band, that was between 500–749 μm and also complete RPE loss that was between 0–250 μm . For this lesion, there were also 3 locations with deep visual sensitivity defects ≤ 10 dB, where 1 was ≤ 0 dB. The sixth example (Fig 3F) shows a lesion with cRORA and also satisfying the criteria for nGA that had more extensive signs of atrophy, including choroidal signal hypertransmission between 750–1000 μm , subsidence of the INL and OPL, and/or hyporeflective wedge-shaped band, that was between 750–1000 μm and complete RPE loss that was between 500–750 μm . This lesion had 8 locations with deep visual sensitivity defects ≤ 10 dB, where 3 were ≤ 0 dB.

Discussion

This study revealed that choroidal signal hypertransmission $\geq 500 \mu\text{m}$, complete RPE loss $\geq 250 \mu\text{m}$, and nGA $\geq 500 \mu\text{m}$, but not RPE attenuation or disruption, were all independently associated with a significant increase in the number of locations with deep visual sensitivity defects that were ≤ 10 dB. When considering RPE and outer retinal atrophy, not all cRORA lesions exhibit a significant difference in the number of deep visual sensitivity defects compared with iRORA lesions, where only lesions with choroidal signal hypertransmission $\geq 500 \mu\text{m}$ and/or complete RPE loss $\geq 250 \mu\text{m}$ showed a significantly higher number of deep visual sensitivity defects compared with iRORA lesions. This study also observed that lesions with only OCT features that define nGA that were $\geq 500 \mu\text{m}$ in extent, irrespective of the presence of hypertransmission $\geq 500 \mu\text{m}$ and/or complete RPE loss $\geq 250 \mu\text{m}$, also had a significantly higher number of locations ≤ 10 dB than regions without. These findings provided the much-needed functional evidence to inform the development of a more granular OCT classification of atrophy in AMD, especially when considering how to define a lesion considered as end-stage atrophy.

The findings of this study build on previous studies suggesting that photoreceptor changes in OCT imaging are associated with reduced visual sensitivity on microperimetry in eyes with GA.^{14–18} Specifically, 2 previous studies reported that regions with EZ disruption showed significantly reduced visual sensitivities when compared with regions without, although EZ disruption was the only parameter examined on OCT imaging.^{14,17} Another study also reported that EZ disruption, along with decreasing full retinal thickness and outer retinal thickness, but not inner retinal

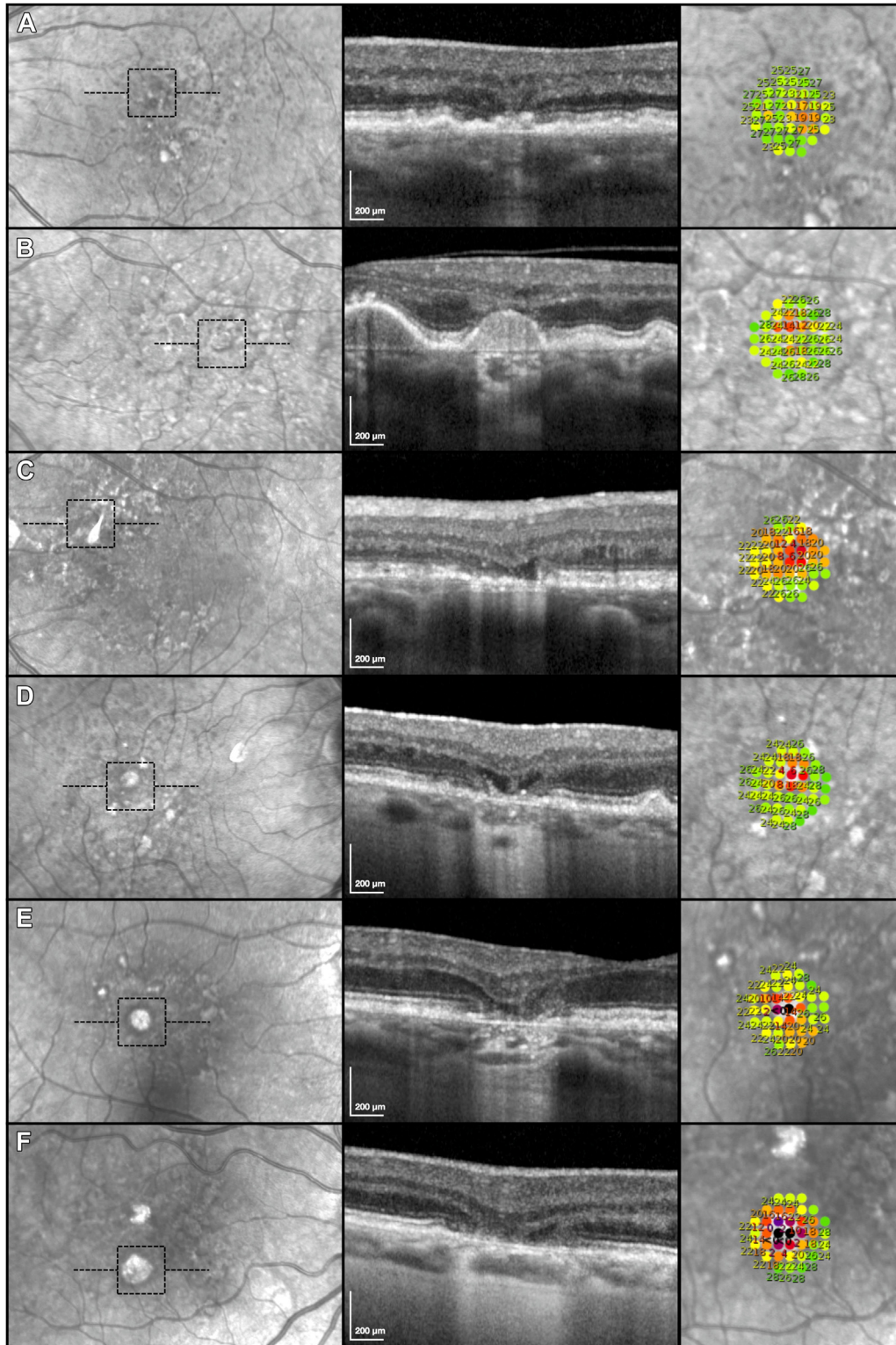


Figure 3. (A-F) Examples of the high-density, targeted microperimetry testing results (right column; region tested indicated by the dashed black boxes on the left column) of lesions that differed in the presence and extent of atrophy seen on OCT B-scans (middle column), location as outlined by horizontal dashed lines in the left column), including choroidal signal hypertransmission, subsidence of the inner nuclear layer and outer plexiform layer and/or presence of a hyporeflective wedge-shaped band within Henle’s fiber layer, and complete retinal pigment epithelium loss (resulting in clear visibility of Bruch’s membrane and without overlying dysmorphic retinal pigment epithelium or debris present). These examples are described in detail in the Results section.

thickness, was associated with reduced visual sensitivities.¹⁵ Similarly, a recent study reported that ONL thickness, full retinal thickness, and inner retina thickness showed the highest feature importance when predicting mesopic visual sensitivities using a machine learning approach.¹⁸ Finally, one previous study by Sayegh et al¹⁶ examined differences in visual sensitivity threshold and the number of absolute scotomas (using MP-1 device [Nidek Technologies, Inc.], which has a more limited dynamic range compared with the device used in this study^{28,29}) across 9 OCT parameters associated with atrophy. They reported that visual sensitivity was only significantly reduced at test locations with ELM disruption compared with those without but that there was no significant difference in visual sensitivity in areas of intense or moderate choroidal signal hypertransmission, complete absence or attenuation of the RPE, intense or moderate RPE thickening at the junctional zone, or OPL thinning or loss. In addition, they reported that the prevalence of absolute scotomas was only significantly higher at test locations with RPE absence or attenuation, ELM loss, or intense thickening of the RPE at the junctional zones of the atrophic lesion. The lack of a significant difference in visual sensitivity and prevalence of absolute scotomas at test locations with choroidal signal hypertransmission reported by Sayegh et al¹⁶ may be due to the lack of quantification of the size of such changes in their analyses because we observed that only regions with choroidal signal hypertransmission $\geq 500 \mu\text{m}$ were associated with a significantly higher number of deep visual sensitivity defects compared with lesions without hypertransmission between 1–249 μm . The findings by Sayegh et al¹⁶ that both regions with only RPE attenuation, as well as those with complete RPE loss, were associated with an increased prevalence of scotomas also differed from the findings of this study and could be potentially attributable to difference in the level of attenuation of the RPE required for this parameter to be deemed present. As we did not quantify the extent of EZ or ELM disruption and ONL thinning (because this was not required when defining the presence of iRORA or cRORA), our study is unable to determine if the number of test locations with deep visual sensitivity defects would vary based on the extent of these OCT parameters of photoreceptor degeneration.^{14–18} However, we observed, for the first time to our knowledge, that the number of deep visual sensitivity defects that were ≤ 10 dB was significantly higher in regions with subsidence of the INL and OPL, and/or hyporeflexive wedge-shaped band within Henle’s fiber layer, that was $\geq 500 \mu\text{m}$ compared with regions without. These findings build upon our previous observations that regions with nGA, defined by the presence of either of these 2 OCT features, were associated with reduced visual sensitivities compared with the neighboring non-atrophic regions, but we did not previously examine the association between the extent of the INL and OPL subsidence and/or hyporeflexive wedge-shaped band and deep visual sensitivity defects.²⁰

The findings of this study suggest that only regions with cRORA that had choroidal signal hypertransmission $\geq 500 \mu\text{m}$ or complete RPE loss $\geq 250 \mu\text{m}$, or these 2 features

together, but not cRORA lesions that only had hypertransmission between 250–499 μm , are associated with a significantly higher number of locations with deep visual sensitivity defects on high-density threshold microperimetry testing compared with regions with iRORA. These findings are especially important when considering how to define a lesion considered as end-stage atrophy and provide functional evidence that not all cRORA lesions will have a dense scotoma.¹¹

Instead, this study observed that hypertransmission $\geq 500 \mu\text{m}$, complete RPE loss $\geq 250 \mu\text{m}$, and features that define nGA $\geq 500 \mu\text{m}$ on OCT imaging were all independently associated with a significant increase in the number of deep visual sensitivity defects ≤ 10 dB. A set of combinations based on an increasing number of each of these 3 features was associated with a progressive increase in the number of deep visual sensitivity defects ≤ 10 dB. However, this set of combinations can be simplified by a set of combinations defined based on the presence of nGA $\geq 500 \mu\text{m}$, with or without choroidal hypertransmission $\geq 500 \mu\text{m}$, and/or complete RPE loss $\geq 250 \mu\text{m}$, and these 2 different sets of combinations were near-identical. This simplification could be achieved as nearly all lesions with only one out of the 3 features associated with deep visual sensitivity defects had nGA $\geq 500 \mu\text{m}$, and because all lesions with 2 out of these 3 features also had nGA $\geq 500 \mu\text{m}$. Based on this simplified set of combinations, regions with nGA $\geq 500 \mu\text{m}$ with either choroidal signal hypertransmission $\geq 500 \mu\text{m}$ or complete RPE loss $\geq 250 \mu\text{m}$, or both features, showed a significantly higher extent of deep visual sensitivity defects that were ≤ 10 dB and ≤ 0 dB than regions without nGA $\geq 500 \mu\text{m}$. This was a similar finding to those based on the presence of cRORA described here. However, we also observed that regions with only nGA $\geq 500 \mu\text{m}$, and without choroidal signal hypertransmission $\geq 500 \mu\text{m}$ and complete RPE loss $\geq 250 \mu\text{m}$, showed a significantly higher number of deep visual sensitivity defects that were ≤ 10 dB, but not ≤ 0 dB, when compared with regions without nGA $\geq 500 \mu\text{m}$.

The evaluation of the number of locations that were ≤ 10 dB provides a more sensitive measure of deep visual sensitivity defects at the floor of the effective dynamic range of the microperimeter used in this study,³¹ rather than ≤ 0 dB at the floor of its physical dynamic range^{28,29} (which is how dense or absolute scotomas are typically defined²⁷). This is because the large degree of measurement variability for locations with such low visual sensitivities^{26,31} would result in fewer test locations with deep visual sensitivity defects that would be considered statistically indistinguishable from absolute scotomas³⁰ (i.e., ≤ 10 dB) to be captured using the cut-off of ≤ 0 dB. These aforementioned findings thus suggest that nGA $\geq 500 \mu\text{m}$ often represents one of the earliest OCT features of an atrophic lesion that is associated with deep visual sensitivity defects ≤ 10 dB.

Limitations of this study include its sample size of 60 eyes from 53 participants, but a strength of this study was the inclusion of a large number of high-density targeted microperimetry tests ($n = 342$) and study visits ($n = 171$) from these participants. Another limitation is the possible

imperfection in the placement of the high-density microperimetry grid on the center of the atrophic lesion, which could be challenging when assessing such localized changes. However, this study only included atrophic lesions that were smaller than the stimulus grid (approximately $\leq 750 \mu\text{m}$), and all tests were reviewed to ensure that the entire atrophic lesion was sampled by the stimulus grid. The use of such a novel high-density targeted microperimetry testing approach was a key strength of this study, providing a highly detailed and comprehensive characterization of the presence of deep visual sensitivity defects of the atrophic lesions that would not be possible with conventional microperimetry testing. Although the findings of this study provide insights into the OCT features in an atrophic lesion that are associated with deep visual sensitivity defects at a global level, future studies are now needed to further examine these associations at a pointwise, local level. Finally, another limitation of this study was the evaluation of deep visual sensitivity defects that were $\leq 10 \text{ dB}$ based on the raw threshold values, rather than using age- and eccentricity-adjusted values. The latter was not possible due to the lack of a well-established normative database,

especially one that is applicable to individualized test locations required for the targeted testing of atrophic lesions performed in this study. However, a previous study showed that locations $\leq 10 \text{ dB}$ represent those at the floor of the effective dynamic range of the microperimetry device used in this study,³¹ and variations in age and eccentricity may thus have a minimal impact on the presence of such deep visual sensitivity defects.

In conclusion, this study demonstrated that not all cRORA lesions exhibit a significant difference in the number of deep visual sensitivity defects when compared with iRORA lesions, and only those with choroidal signal hypertransmission $\geq 500 \mu\text{m}$ and/or complete RPE loss $\geq 250 \mu\text{m}$ showed a significantly greater number of deep visual sensitivity defects. It also revealed that lesions with nGA $\geq 500 \mu\text{m}$ in extent, irrespective of hypertransmission $\geq 500 \mu\text{m}$ and complete RPE loss $\geq 250 \mu\text{m}$, showed a significantly higher number of deep visual sensitivity defects $\leq 10 \text{ dB}$ when compared with lesions where it was absent. These findings thus provide the much-needed functional evidence to help define an end-stage atrophic lesion that would be associated with deep visual sensitivity defects.

Footnotes and Disclosures

Originally received: September 25, 2023.

Final revision: October 19, 2023.

Accepted: November 1, 2023.

Available online: November 4, 2023. Manuscript no. XOPS-D-23-00233R1.

¹ Centre for Eye Research Australia, Royal Victorian Eye and Ear Hospital, East Melbourne, Australia.

² Ophthalmology, Department of Surgery, The University of Melbourne, Melbourne, Australia.

Disclosure(s):

All authors have completed and submitted the ICMJE disclosures form.

The author(s) have made the following disclosure(s): R.H.G.: Personal fees – Roche/Genentech, Bayer, Novartis, and Apellis outside the submitted work.

The other authors have no proprietary or commercial interest in any materials discussed in this article.

Supported by the National Health and Medical Research Council of Australia (#2008382 [Z.W.] and #1194667 [R.H.G.]), the BrightFocus Foundation (#M2019073 [Z.W. and R.H.G.]). CERA receives operational infrastructure support from the Victorian Government. The funders had no role in the manuscript writing and the decision to submit the manuscript for publication.

HUMAN SUBJECTS: Human subjects were included in this study. This study was conducted in accordance with the tenets of the Declaration of Helsinki and the International Conference on Harmonization Guidelines for

Good Clinical Practice. Institutional review board approval was obtained for this study and the participants enrolled all provided informed consent.

No animal subjects were used in this study.

Author Contributions:

Conception and design: Wu, Guymer

Data collection: Wu, Glover, Gee, Hodgson, Guymer

Analysis and interpretation: Wu, Guymer

Obtained funding: Wu, Guymer

Overall responsibility: Wu, Guymer

Abbreviations and Acronyms:

AMD = age-related macular degeneration; **cRORA** = complete RPE and outer retinal atrophy; **dB** = decibels; **ELM** = external limiting membrane; **EZ** = ellipsoid zone; **GA** = geographic atrophy; **INL** = inner nuclear layer; **iRORA** = incomplete RPE and outer retinal atrophy; **MAIA** = Macular Integrity Assessment; **nGA** = nascent geographic atrophy; **ONL** = outer nuclear layer; **OPL** = outer plexiform layer; **RPE** = retinal pigment epithelium.

Keywords:

cRORA, Nascent Geographic Atrophy, Microperimetry, Age-Related Macular Degeneration, Visual Field Tests.

Correspondence:

Zhichao Wu, BAppSc(Optom), PhD, Level 7, 32 Gisborne Street, East Melbourne, VIC 3002, Australia. E-mail: wu.z@unimelb.edu.au.

References

- Sarks JP, Sarks SH, Killingsworth MC. Evolution of geographic atrophy of the retinal pigment epithelium. *Eye (Lond)*. 1988;2:552–577. <https://doi.org/10.1038/eye.1988.106>.
- Kim SY, Sadda S, Humayun MS, et al. Morphometric analysis of the macula in eyes with geographic atrophy due to age-related macular degeneration. *Retina*. 2002;22:464–470. <https://doi.org/10.1097/00006982-200208000-00011>.
- Bhutto I, Luty G. Understanding age-related macular degeneration (AMD): relationships between the photoreceptor/retinal pigment epithelium/Bruch's membrane/choriocapillaris

- complex. *Mol Aspects Med.* 2012;33:295–317. <https://doi.org/10.1016/j.mam.2012.04.005>.
4. Bird AC, Phillips RL, Hageman GS. Geographic atrophy: a histopathological assessment. *JAMA Ophthalmol.* 2014;132:338–345. <https://doi.org/10.1001/jamaophthalmol.2013.5799>.
 5. Li M, Dolz-Marco R, Huisinck C, et al. Clinicopathologic correlation of geographic atrophy secondary to age-related macular degeneration. *Retina.* 2019;39:802–816. <https://doi.org/10.1097/IAE.0000000000002461>.
 6. Fleckenstein M, Charbel Issa PC, Helb HM, et al. High-resolution spectral domain-OCT imaging in geographic atrophy associated with age-related macular degeneration. *Invest Ophthalmol Vis Sci.* 2008;49:4137–4144. <https://doi.org/10.1167/iovs.08-1967>.
 7. Bearely S, Chau FY, Koreishi A, Stinnett SS, Izatt JA, Toth CA. Spectral domain optical coherence tomography imaging of geographic atrophy margins. *Ophthalmology.* 2009;116:1762–1769. <https://doi.org/10.1016/j.ophtha.2009.04.015>.
 8. Schmitz-Valckenberg S, Fleckenstein M, Göbel AP, et al. Optical coherence tomography and autofluorescence findings in areas with geographic atrophy due to age-related macular degeneration. *Invest Ophthalmol Vis Sci.* 2011;52:1–6. <https://doi.org/10.1167/iovs.10-5619>.
 9. Sayegh RG, Simader C, Scheschy U, et al. A systematic comparison of spectral-domain optical coherence tomography and fundus autofluorescence in patients with geographic atrophy. *Ophthalmology.* 2011;118:1844–1851. <https://doi.org/10.1016/j.ophtha.2011.01.043>.
 10. Sadda SR, Guymer R, Holz FG, et al. Consensus definition for atrophy associated with age-related macular degeneration on OCT: Classification of Atrophy Report 3. *Ophthalmology.* 2018;125:537–548. <https://doi.org/10.1016/j.ophtha.2017.09.028>.
 11. Guymer RH, Rosenfeld PJ, Curcio CA, et al. Incomplete retinal pigment epithelial and outer retinal atrophy in age-related macular degeneration: classification of Atrophy Meeting Report 4. *Ophthalmology.* 2020;127:394–409. <https://doi.org/10.1016/j.ophtha.2019.09.035>.
 12. Pfau M, Jolly JK, Wu Z, et al. Fundus-controlled perimetry (microperimetry): application as outcome measure in clinical trials. *Prog Retin Eye Res.* 2021;82:100907. <https://doi.org/10.1016/j.preteyeres.2020.100907>.
 13. Rohrschneider K, Bültmann S, Springer C. Use of fundus perimetry (microperimetry) to quantify macular sensitivity. *Prog Retin Eye Res.* 2008;27:536–548. <https://doi.org/10.1016/j.preteyeres.2008.07.003>.
 14. Querques L, Querques G, Forte R, Souied EH. Microperimetric correlations of autofluorescence and optical coherence tomography imaging in dry age-related macular degeneration. *Am J Ophthalmol.* 2012;153:1110–1115. <https://doi.org/10.1016/j.ajo.2011.11.002>.
 15. Pilotto E, Benetti E, Convento E, et al. Microperimetry, fundus autofluorescence, and retinal layer changes in progressing geographic atrophy. *Can J Ophthalmol.* 2013;48:386–393. <https://doi.org/10.1016/j.cjjo.2013.03.022>.
 16. Sayegh RG, Kiss CG, Simader C, et al. A systematic correlation of morphology and function using spectral domain optical coherence tomography and microperimetry in patients with geographic atrophy. *Br J Ophthalmol.* 2014;98:1050–1055. <https://doi.org/10.1136/bjophthalmol-2014-305195>.
 17. Takahashi A, Ooto S, Yamashiro K, et al. Photoreceptor damage and reduction of retinal sensitivity surrounding geographic atrophy in age-related macular degeneration. *Am J Ophthalmol.* 2016;168:260–268. <https://doi.org/10.1016/j.ajo.2016.06.006>.
 18. Pfau M, von der Emde L, Dysli C, et al. Determinants of cone and rod functions in geographic atrophy: AI-based structure-function correlation. *Am J Ophthalmol.* 2020;217:162–173. <https://doi.org/10.1016/j.ajo.2020.04.003>.
 19. Wu Z, Luu CD, Ayton LN, et al. Optical coherence tomography-defined changes preceding the development of drusen-associated atrophy in age-related macular degeneration. *Ophthalmology.* 2014;121:2415–2422. <https://doi.org/10.1016/j.ophtha.2014.06.034>.
 20. Wu Z, Ayton LN, Luu CD, Guymer RH. Microperimetry of nascent geographic atrophy in age-related macular degeneration. *Invest Ophthalmol Vis Sci.* 2014;56:115–121. <https://doi.org/10.1167/iovs.14-15614>.
 21. Wu Z, Luu CD, Ayton LN, et al. Fundus autofluorescence characteristics of nascent geographic atrophy in age-related macular degeneration. *Invest Ophthalmol Vis Sci.* 2015;56:1546–1552. <https://doi.org/10.1167/iovs.14-16211>.
 22. Ferrara D, Silver RE, Louzada RN, et al. Optical coherence tomography features preceding the onset of advanced age-related macular degeneration. *Invest Ophthalmol Vis Sci.* 2017;58:3519–3529. <https://doi.org/10.1167/iovs.17-21696>.
 23. Wu Z, Luu CD, Hodgson LAB, et al. Prospective longitudinal evaluation of nascent geographic atrophy in age-related macular degeneration. *Ophthalmol Retina.* 2020;4:568–575. <https://doi.org/10.1016/j.oret.2019.12.011>.
 24. Wu Z, Goh KL, Hodgson LAB, Guymer RH. Incomplete retinal pigment epithelial and outer retinal atrophy: longitudinal evaluation in age-related macular degeneration. *Ophthalmology.* 2023;130:205–212. <https://doi.org/10.1016/j.ophtha.2022.09.004>.
 25. Wu Z, Ayton LN, Guymer RH, Luu CD. Intrasession test-retest variability of microperimetry in age-related macular degeneration. *Invest Ophthalmol Vis Sci.* 2013;54:7378–7385. <https://doi.org/10.1167/iovs.13-12617>.
 26. Wu Z, Hadoux X, Jannaud M, et al. Systematic underestimation of visual sensitivity loss on microperimetry: implications for testing protocols in clinical trials. *Transl Vis Sci Technol.* 2023;12:11. <https://doi.org/10.1167/tvst.12.7.11>.
 27. Csaky KG, Patel PJ, Sepah YJ, et al. Microperimetry for geographic atrophy secondary to age-related macular degeneration. *Surv Ophthalmol.* 2019;64:353–364. <https://doi.org/10.1016/j.survophthal.2019.01.014>.
 28. Wong EN, Mackey DA, Morgan WH, Chen FK. Inter-device comparison of retinal sensitivity measurements: the CenterVue Maia and the Nidek MP-1. *Clin Exp Ophthalmol.* 2016;44:15–23. <https://doi.org/10.1111/ceo.12629>.
 29. Xu L, Wu Z, Guymer RH, Anderson AJ. Investigating the discrepancy between Maia and MP-1 microperimetry results. *Ophthalmic Physiol Opt.* 2021;41:1231–1240. <https://doi.org/10.1111/opo.12877>.
 30. Wall M, Woodward KR, Doyle CK, Zamba G. The effective dynamic ranges of standard automated perimetry sizes III and V and motion and matrix perimetry. *Arch Ophthalmol.* 2010;128:570–576. <https://doi.org/10.1001/archophthalmol.2010.71>.
 31. Pfau M, Lindner M, Müller PL, et al. Effective dynamic range and retest reliability of dark-adapted two-color fundus-controlled perimetry in patients with macular diseases. *Invest Ophthalmol Vis Sci.* 2017;58:10158–10167. <https://doi.org/10.1167/iovs.17-21454>.